HHS Public Access

Author manuscript

Nat Neurosci. Author manuscript; available in PMC 2010 December 01.

Published in final edited form as:

Nat Neurosci. 2010 June ; 13(6): 708–714. doi:10.1038/nn.2552.

Temperature-induced opening of TRPV1 ion channel is stabilized by the pore domain

Jörg Grandl[1], **Sung Eun Kim**[1], **Valerie Uzzell**[1,*], **Badry Bursulaya**[2], **Matt Petrus**[2], **Michael Bandell**[2], and **Ardem Patapoutian**[1,2,3]

[1] Department of Cell Biology, The Scripps Research Institute, La Jolla, CA 92037, USA.

[2] Genomics Institute of the Novartis Research Foundation, San Diego, CA 92121, USA.

Summary

TRPV1 is the founding and best-studied member of the family of temperature-activated transient receptor potential ion channels (thermoTRPs). Voltage, chemicals, and heat amongst other agonists allosterically gate TRPV1. Molecular determinants for TRPV1 activation by capsaicin, allicin, acid, ammonia, and voltage have been identified. However, the structures and mechanisms mediating its pronounced temperature-sensitivity remain unclear. Recent studies of the related channel TRPV3 identified residues within the pore region required for heat activation. Here we use both random and targeted mutagenesis screens of TRPV1 and identify point mutations in the outer pore region that specifically impair temperature-activation. Single channel analysis shows that TRPV1 mutations disrupt heat-sensitivity by ablating long channel openings, that are part of the temperature-gating pathway. We propose that sequential occupancy of short and long open states upon activation provides a mechanism to enhance temperature-sensitivity. Our study suggests that the outer pore plays a general role in heat-sensitivity of thermoTRPs.

Somatosensory neurons sense changes in our environment through neuronal endings in the skin. A group of non-selective transient receptor potential (TRP) cation channels are expressed in somatosensory neurons, have emerged as major sensors of temperature and chemicals, and have been implicated in acute and chronic pain1-2. TRPV1, the founding member of thermoTRPs, is activated under physiological conditions by noxious high temperatures (>42°C), low (extracellular) and high (intracellular) pH, positive voltages, and by pungent chemicals including capsaicin - the active ingredient in hot chili peppers3-7. A role for TRPV1 in acute noxious thermosensation and thermal hyperalgesia in-vivo is well-documented8-9. TRPV1 is one of nine known mammalian thermoTRPs, each of which is activated with a distinct temperature-threshold10-18.

[3] Corresponding author, apatapou@gnf.org.

[*] Present address: *Illumina Inc., San Diego, CA 92121, USA.*

Author contributions J.G. designed the study, collected and analyzed data and wrote the manuscript. S.E.K. collected and analyzed data in the primary screen. V.U. prepared the mutant library, collected and analyzed data in the primary screen. B.B. performed molecular modeling. M.P. prepared the mutant library. M.B. developed the screening conditions. A.P. designed the study and edited the manuscript. All authors discussed results and commented on the manuscript.

Mutagenesis studies have been used to map residues in TRPV1 that are specifically implicated in activation by capsaicin, allicin, protons, ammonia, and voltage3,19-24. In contrast, temperature-gating in thermoTRPs remains unclear. It has been shown that temperature-sensitivity in heat-activated TRPV1 and cold-activated TRPM8 is allosterically linked to chemical- and voltage-activation7,25-28. Furthermore, chimeric TRPV1/TRPM8 constructs have shown that the cytoplasmic C-terminal domains can set temperature-directionality29. However, an established and unifying theory of temperature-gating is still elusive.

Recently, we successfully used an unbiased mutagenesis screen on related TRPV3. We identified single-point mutations clustered in TM6 and the adjacent extracellular loop that rendered TRPV3 temperature-insensitive, without interfering with its mechanisms of ligand-activation30. However, how these mutations affect channel function mechanistically and whether these residues are specifically required for TRPV3 or are part of a general structure implicated in temperature-sensitivity of thermoTRPs is unknown. This prompted us to apply the same method to TRPV1, a closely related ion channel, and the best-characterized thermoTRP biophysically.

Two screens yield temperature-specific point-mutations

We used two mutant libraries to search for point mutations that alter activation of TRPV1 by high temperature, but not by chemical agonists or low pH. First, in an unbiased approach, we constructed a large (~8500) library of randomly mutated TRPV1 clones containing ~2 amino-acid changes per clone. Second, we engineered a focused and nearly-saturated library by randomizing 9 TRPV1 residues that aligned with temperature-specific point-mutations that we identified previously in the pore region of TRPV3 (Fig. 1a). Both mutant libraries were assayed in a high-throughput calcium-influx assay on transiently-transfected HEK293 cells for their responses to heat (45°C), capsaicin (100 nM) and acidic buffer (pH 6.6) independently. We additionally measured responses to cold temperatures (10°C) in an attempt to identify mutants with inversed temperature-activation, based on results from the TRPV1/TRPM8 chimeric studies29. We subsequently selected for clones that showed a significant change in response for one stimulus, while maintaining wild-type-like responses for at least one other activation mechanism (see Methods for details).

We identified one previously known single-point mutation (E600V) causing complete and specific loss of pH-sensitivity21 (Supplementary Fig. 1). Another mutation (F489Y) resulted in a rightward shift of the capsaicin-EC_{50} (~2.5-fold), likely caused by its close proximity to a domain shown to be implicated in capsaicin-sensitivity20 (Supplementary Fig. 1). These findings validate our general approach, mutant library, and selection criteria to identify stimulus-specific residues.

While none of the clones responded to cold stimulation, we found one single point-mutation from the random library (N628K) and two from the focused library (N652T and Y653T) that result in TRPV1 channels that respond normally to capsaicin and pH, but cause a heat-response that is reduced in amplitude and shifted to higher temperatures (Fig. 1a-e and Table 1). Moreover, the time-course of activation of these single point mutants was identical

(capsaicin and 2APB) or very similar (pH) when compared to wild-type TRPV1, suggesting that desensitization is not strongly altered (Supplementary Fig. 2).

The temperature deficits in TRPV1 clones were mild compared to point mutants we identified in TRPV330. We therefore tested if combination of these mutations can enhance the temperature-phenotype. We therefore engineered a 'double-mutant' carrying mutations N652T+Y653T and a 'triple-mutant' with mutations N628K+N652T+Y653T. Strikingly, combining these mutations yielded receptors with capsaicin-, 2APB- and pH-EC_{50}-values and maximal responses indistinguishable from wild-type TRPV1 (Fig. 1b and Table 1), but with further reduction in temperature-responses (Fig. 1c-e). Whole-cell recordings confirmed the deficit in temperature-response seen in FLIPR experiments (Fig. 1e).

Both TRPV1 mutants from the targeted library (N652 and Y653) are in the presumptive extracellular loop between the selectivity filter and TM6 (Fig. 2a,b). None of the TM6 mutations from TRPV3 came up positive for TRPV1. Remarkably, the sole mutation obtained from the random library (N628) is also in the pore region - adjacent to the pore helix, and potentially in the loop joining TM5 to the pore helix (Fig. 2a,b). Interestingly, in a homology model of the TRPV1 pore domain based on the crystal structure of the homologous Kv1.2 (46% homology in pore regions)31, these residues are in close proximity to each other in adjacent subunits (N628 to N652/Y653), and within proximity and potential direct contact to three glutamates (E600, E648 and E651) previously found to be important for pH-activation21-22 (Supplementary Fig. 3). Thus, the entry of the TRPV1 pore consists of a dense accumulation of residues important for these two modalities.

Mutations diminish temperature-shift of voltage-activation

We were unable to test the effect of temperature mutations on voltage in TRPV3, since this ion channel is only modulated by voltage (voltage is not sufficient to activate TRPV3). We therefore tested how the modality of voltage is affected in the TRPV1 single- (N628K), double- (N652T+Y653T), and triple-mutant (N628K+N652T+Y653T) that cause the strongest temperature phenotype. In wild-type TRPV1 the maximum current increases and the voltage of half-maximal activation (V_{half}) is shifted to more negative potentials by capsaicin and higher temperatures7,25,27-28. We therefore measured channel activation in the absence and presence of capsaicin and also at different temperatures while applying a voltage-step protocol. In un-normalized current-voltage (*I*-V) plots, positive potentials (>100 mV) at 20°C evoke a current in wild-type TRPV1 and the triple-mutant (N628K+N652T +Y653T) (Fig. 3a). We found that all heat mutant channels are activated with a V_{half} indistinguishable from wild-type TRPV1 channels (wild-type TRPV1: 161 ± 15 mV, N628K: 157 ± 6 mV, N652T+Y653T: 146 ± 38 mV, N628K+N652T+Y653T: 157 ± 19 mV), which can be seen best in conductance-voltage (*G*-V) plots (Fig. 3b,c). Application of a saturating capsaicin concentration (1 μM) at 20°C shifted the voltage-activation curve of all mutants indistinguishably when compared to wild-type TRPV1 (no capsaicin: 161 ± 15 mV; 1 μM capsaicin: 54 ± 23 mV) (Fig. 3a-c). Hence, voltage response and the capsaicin-induced voltage-shift are intact in these channels at room temperature. However, the current evoked at very positive potentials (>100 mV) increased dramatically with higher temperature in wild-type TRPV1, but hardly in the triple-mutant (N628K+N652T+Y653T)

(Fig. 3d-f). This observation confirms the deficit in temperature-activation observed for this mutant in the calcium-influx assay. Strikingly, in all three mutants examined, higher temperatures shifted the V_{half} compared to 20°C to a smaller extent than observed in wild-type channels (Fig. 3d-f). This is most clearly observed for shifts of V_{half} values evoked by 40°C (wild-type TRPV1: −81 ± 23 mV, N628K: −37 ± 7 mV, N652T+Y653T: −37 ± 30 mV, N628K+N652T+Y653T: 7 ± 3 mV), and the decrease of shifts of V_{half} correlates with the magnitude of deficit of the mutants in temperature-activation (ET_{50}): wild-type TRPV1 < N628K < N652T+Y653T < N628K+N652T+Y653T (Fig. 1d and Fig. 3d-f). Remarkably, the triple-mutant (N628K+N652T+Y653T) does not exhibit any significant shift of V_{half} (155 ± 20 mV at 20°C vs. 162 ± 30 mV at 40°C) in the tested range, which was limited by the temperature-stability of gigaseal patches. Therefore, allosteric coupling of capsaicin-voltage is normal (at 20°C), but the temperature-voltage coupling is changed, reinforcing that mutations identified are specifically affecting the temperature-modality.

Mutations ablate long channel openings

Calcium-flux and whole-cell patch-clamp measurements suggest that mutations severely affect temperature-activation, but do not completely ablate it, while activation by voltage and capsaicin remain unaltered. The current *I* measured over a whole cell is determined by the number of channels N, the unitary conductance *i* and the probability of channel opening p_o: $I = N \cdot i \cdot p_o$. Knowing which parameter is altered might help understand how mutations affect temperature-gating mechanistically. It is reasonable to assume that the number of channels (N) is not changed, since mutant channels have wild-type-like maximal responses to capsaicin, 2APB and acid. However, the identified mutations are located near the pore and thus an alteration of the unitary conductance is a possibility. To gain information on unitary conductance and channel gating kinetics we recorded single-channel activity in the cell-attached configuration of the mutant with the strongest temperature-phenotype (N628K +N652T+Y653T) and compared it to wild-type TRPV1. In TRPV1 wild-type we observed occasional single channel openings shown by brief outward current pulses at +100 mV from the baseline that were absent in non-transfected cells and that became more frequent at higher temperatures (10°C < 20°C < 30°C) (Fig. 4a and Supplementary Fig. 4), which has been previously described32. Recordings of the triple-mutant (N628K+N652T+Y653T) also showed an increase in channel activity at elevated temperatures, which confirms our previous observation (see Fig. 1) that even the triple-mutant (N628K+N652T+Y653T) retained some temperature-sensitivity (Fig. 4a and Supplementary Fig. 4). However, we observed that the gating kinetics differed dramatically at all temperatures: whereas wild-type TRPV1 was gated in short spikes (~1 ms) and longer (~10 ms) openings, open-times of the triple mutant (N628K+N652T+Y653T) were much shorter (~ 1ms) (Fig. 4a and Supplementary Fig. 4). In both cases, the unitary conductance was identical (TRPV1: 87 ± 2 pS, N628K+N652T+Y653T: 84 ± 7 pS; at +100 mV; 20°C) (Fig. 4b). In addition, we found the unitary conductance of wild-type TRPV1 to be weakly temperature-dependent ($Q_{10}(i)$ = 1.4 ± 0.1), which is expected from the temperature-dependence of the diffusion of ions in aqueous solution and had been shown previously (Fig. 4c)7,33.

We recorded channel activity at moderate temperatures (10°C–30°C) to increase patch-stability and thereby the number of gating events used for statistical analysis. As a result, for

each temperature, 20.000–60.000 gating events could be recorded and analyzed. The difference in gating kinetics is quantified by open-time histograms that show peaking frequencies of wild-type TRPV1 channel openings of short (<1 ms) and longer (~10 ms) durations, the latter of which is completely absent in the triple-mutant (N628K+N652T +Y653T) which is solely open in the 1 ms time-range (Fig. 4d). Thus, we conclude that the alteration in the temperature-activation observed on the whole-cell level is due to a shift in the gating-equilibrium at all temperatures, resulting in a loss of longer open-times.

As a control, we recorded traces in the presence of capsaicin and at −100 mV (to minimize voltage-gating). Capsaicin-activation has been previously described to cause rapid fluctuations between different conductance levels34. In addition, open-time histograms suggest at least three distinct open-states, presumably originating from partially and fully-liganded channels35. In our recordings both wild-type TRPV1 and the triple-mutant (N628K +N652T+Y653T) showed activity that was identical in conductance and kinetics (Supplementary Fig. 5a). The multiple and relatively small conductance levels prevented us from calculating dwell-time histograms to compare the two receptors more quantitatively. We therefore recorded channel activity of both wild-type TRPV1 and the triple-mutant (N628K+N652T+Y653T) at +100mV (in these conditions TRPV1 is gated in a unique large conductance) induced by a non-saturating concentration of capsaicin (100 nM) under conditions that minimize activation by temperature (10°C) (Supplementary Fig. 5b). These recordings show that, within the limits of the filter frequency of 2.9 kHz, gating kinetics and histograms of open- and-closed times are virtually identical between wild-type and mutant TRPV1, and confirm that the triple mutant is normally gated by capsaicin.

Multiple open states alter the P_o and possibly the Q_{10}

The heterogeneous open-time histograms (Fig. 4d) demonstrate that wild-type TRPV1 temperature-gating involves multiple kinetically distinct open states (short and long). Mutations in the pore domain ablate the ability to transition to the population of longer, more stable open states, possibly by destabilizing long-lasting open conformations. This lack of long open times decreases the open probability (P_o). How the multiple open states can be accessed from one or possibly an ensemble of multiple closed states and how they are functionally related is unclear. Since all open states are conducting states with the same unitary conductance *i*, it is plausible that they are structurally similar and likely direct transitions occur between them. Importantly, sequential transition between multiple open states generates a higher temperature-sensitivity (Q_{10}) than provided by one temperature-dependent transition alone. In this hypothetical mechanism the temperature-dependence of the overall current (*I*) is the product of the temperature-dependence of the unitary conductance and the temperature-dependencies of all individual sequential gating transitions (Q_n): $Q_{10}(I) = Q_{10}(i) \cdot \pi\, Q_{10}(\mathrm{On})$. The lack of long open times in our mutants is thus consistent with the decreased temperature sensitivity we observe. In summary we conclude, that the pore domain of wild-type TRPV1 is essential to stabilize the channel in a conducting state, thereby increasing the overall-open probability and temperature-sensitivity of the total current upon temperature-activation.

Discussion

In this study, we set out to map residues in TRPV1 that are uniquely required for temperature-gating. At first, this endeavor might seem counterintuitive, since temperature (unlike a chemical) is not spatially confined36. However, the effect temperature exerts on the tertiary and quaternary structure of a protein is generally not uniform37, and structural changes involved in the temperature gating-reaction might be localized. This idea is supported by the concurrent finding that the pore turret of TRPV1 undergoes structural changes that are temperature-dependent, but not voltage- or capsaicin-dependent38.

The unbiased screen identified one residue with a temperature-specific phenotype. In addition, the targeted library yielded two positions. It is clear that screening 8,500 clones (which represents on average 20 mutations per amino acid residue, see Methods) of randomly mutagenized library does not achieve saturation. The targeted library clearly complements the random approach. For example, position Y653 identified in the target library causes a temperature-specific phenotype in only 1 of 19 possible substitutions (see Methods), and was not picked up in the random library. Therefore, it is very unlikely that we have identified all heat-specific mutations of TRPV1. Furthermore, domains involved in capsaicin- and pH-gating might substantially overlap with a hypothetical temperature-domain and hence mutations within it might not be temperature-specific. This is likely to be a reason why some of the other functional mutations known for TRPV1 were not identified here. For example, the acid-related residue E648 also affects capsaicin-activation when mutated to glutamine, but not alanine and would therefore not have been identified as agonist-specific in our screen21. Regardless of these limitations, the screen succeeded by identifying some of the known residues/domains for capsaicin, acid-activation, and three temperature-mutations allowing biophysical analysis of these mutants.

Similar to TRPV3, the mutations we found are located in the pore-region, suggesting that the pore-domain plays a general role for temperature-gating in TRPVs. Of course, it could be argued that the focused library only allowed hits to be found in the pore-region. Still, no mutation outside the pore-region was identified among ~8500 clones covering the entire protein. It is also important to note that the residues implicated in TRPV1 and TRPV3 are not completely overlapping. This, together with a lack of mechanistic understanding of the temperature insensitivity of TRPV3 mutants (which show a complete loss of temperature response) raises the possibility that temperature has structurally distinct effects on these two homologous channels, and that the pore domain plays disparate roles in temperature sensitivity.

Another striking aspect of the location of the temperature mutations in TRPV1 is their close proximity to residues mediating pH-sensitivity21-22. Specifically, the temperature-phenotype in N628 only occurred when it was mutated to the positively charged amino-acids arginine and lysine (see Methods), further highlighting a possible interaction with the negative charge at E600. However, it is important to note that the molecular model of the TRPV1 pore might be inaccurate in predicting the direct contact of residue N628 (temperature) to E600 (pH) across subunits21-22. Indeed, alternative homology models have been proposed that do not suggest this proximity39. Regardless, the proximity of N652/

Y653 (temperature) to E648/E651 (pH) is obvious, and again raises the hypothesis that structural changes induced by heat and pH are similar and might eventually converge to gate TRPV121. Recently-reported overall gain-of-function mutations located in the pore-domain supports this idea40.

The single- and combined-mutant channels analyzed here are normally activated by capsaicin, 2APB, pH and have normal V_{half} values at 20°C, but have reduced or ablated temperature-response and temperature-induced voltage-shifts characteristic for wild-type TRPV17,25. This might not be surprising, since our screen selected for normal channel function at room-temperature and a loss-of-function phenotype at high temperature. Sharp temperature-thresholds that are characteristic for all thermoTRPs cannot be readily translated to the single-channel level, where channel-activity occurs at all temperatures, only at altered probabilities. At all temperatures tested (10°C, 20°C and 30°C), the open-probability in the strongest mutant (N628K+N652T+Y653T) is reduced and single-channel recordings show that this is due to a shifted gating-equilibrium and not unitary conductance.

Most importantly, our single-channel recordings demonstrate that these mutations strongly influence the stability of long, but not short open states. Therefore, temperature-gating is possibly a multi-step process that involves distinct residues, partially independent from those required by other agonists (capsaicin and pH). This mechanism differs from previous descriptions of temperature-gating as an apparent one-step mechanism between one open and one closed state7. A one-step gating-reaction describes the activation observed on the whole-cell level sufficiently well, likely because some open states are very short and not rate-limiting, and thus does not contribute significantly to the overall open-probability. However, a one-step mechanism cannot explain the complex gating observed in single-channel recordings and how mutations specifically affect a single open state. Certainly, a sequential two-step mechanism is again oversimplified, since it does not account for other agonists like capsaicin, voltage or acid. In addition, multiple structural conformations might not be kinetically distinguishable and therefore not represented. And finally, multiple closed states might be functionally relevant during the temperature-activation process. However, this hypothetical mechanism demonstrates that extreme temperature-sensitivity might be generated by sequential mildly temperature-sensitive steps.

Our work raises the possibility that pore-loops are integral structures for thermo-sensitivity of all thermoTRPs, and the analysis of the heat-deficient mutants provided a structural correlate for the function of temperature-sensitivity in TRPV1. Our model for temperature gating critically depends on experimental data of mutants that are specifically deficient in a single gating step. Therefore, the combination of in-depth analysis of wild-type channel function combined with analysis of temperature-deficient mutants from a high-throughput screen has enabled us to advance our mechanistic understanding of temperature-sensitivity of ion channels.

Methods

Mutant Libraries

Generation of mutant libraries is as described30,41. For the random large-scale library, error prone PCR was performed with the full-length rat TRPV1 gene (Diversify PCR random mutagenesis kit, Clontech). Subsequently, mutagenized DNA was digested with HindIII +Sac2 or Sac2+NotI and ligated into digested rTRPV1-pcDNA5 vectors. This generated two separate mutant libraries (1–448 a.a. and 449–838 a.a.) and sequencing of 10 clones yielded a mutation-frequency of ~2 a.a./clone. About 4400 colonies were picked for each library and grown 12 h in 96-deep-well plates containing 1.6 ml of TB/well. Subsequently, plasmid DNA was isolated using the Nucleospin Robot-96 plasmid kit (Macherey-Nagel) and DNA was normalized to 40 ng/μl using a 96-well UV spectrophotometer and an automated pipetting station (MWG Biotech).

For the focused, saturating library QuikChange II XL Site-directed Mutagenesis Kit (Stratagene) was used together with primers that randomized the three nucleotides (NNN) coding for the targeted amino acids. The alignment of amino-acid sequences between rat TRPV1 and mouse TRPV3 was made with ClustalW. The mutated positions of TRPV1 are: Glu648, Phe649, Asn652, Tyr653, Lys656, Phe659, Leu662, Tyr666 and Ile668 (Fig. 1a). For each reaction, 48 transformants were picked, grown, DNA isolated and normalized as described above.

Cell-culture/Transfection

Transfection of mutant libraries has been described before30,41. Using a Hewlett Packard Minitrak devise we plated DNA in quadruplicate into poly-D-lysine-coated 384-well clear-bottom assay plates (Greiner) at 75 ng/well. Positive (wild-type TRPV1) and negative (pcDNA5) assay controls were included. Transfections were done by adding Fugene 6.0 (Roche) (0.2 μl/well) diluted in OPTI-MEM (Invitrogen) and trypsinized HEK293T cells (8000 cells/well) to all wells. Transfected HEK293 cells were grown at 37°C, 5% CO_2 in Dulbecco's minimal essential medium containing 4.5 mg/ml glucose, 10% heat-inactivated fetal bovine serum, 50 units/ml penicillin, and 50 μg/ml streptomycin.

Screen

Two days after transfection cells were washed with HANKS buffer using an M384 Atlas microplate washer (Titertek), loaded with the calcium-sensitive fluorophore Fluo-3 (Molecular Devices) for 1.5 h, washed again and transferred to a FLIPR-TETRA plate-reader (Molecular Devices) to monitor fluorescence. Separate screens were performed using heat/cold-stimulation30 (25°C to 45°C and 25°C to 10°C), or addition of buffer containing capsaicin (100 nM, final concentration) or buffer adjusted to low pH (6.6, final pH). Focused, saturating libraries were additionally screened with 2APB (100 μM), camphor (3.9 mM) and NH_4Cl (300 mM). All stock solutions were made in DMSO and concentrations were tested before to evoke ~90% of maximal responses in wild-type TRPV1.

Data-analysis of library screens

Maximal fluorescence responses were calculated for each well after baseline subtraction. For wells containing TRPV1 wild-type and pcDNA all data (n=360, large screen; n=20 focused screen) were pooled across plates to calculate average maximum (mean) and standard deviation (σ), for each stimulus. Data-analysis was performed using routines written in Matlab and Igor Pro (Wavemetrics).

For the large-scale library clones were selected as specific if 3 or 4 wells responded normally ($mean_{V1} - 1.28 \cdot \sigma_{V1} < response < mean_{V1} + 1.28 \cdot \sigma_{V1}$) to at least one, but significantly differently ($response < mean_{V1} - 2.58 \cdot \sigma_{V1}$ or $response > mean_{V1} + 2.58 \cdot \sigma_{V1}$) to another stimulus. For hit-validation, 884 clones were initially selected, regrown for DNA isolation and assayed as described above. 33 clones were confirmed as hits, fully sequenced, Maxi-prep DNA prepared and subsequently EC_{50} curves (capsaicin, pH) and temperature-responses measured. For measuring pH-evoked responses HANKS buffer adjusted to different low pH values was used. Separately, equal volumes of low-pH buffer were added to standard HANKS buffer and the resulting pH measured to calibrate dose-response curves. Single-point mutations of all identified alterations were engineered, clones sequenced and tested again with full dose-responses and compared against wild-type TRPV1 as described above. Only mutation of amino-acid N628 qualified as a final hit. In order to find the strongest phenotype we subsequently mutated N628 into all other 19 amino-acids and tested full dose-responses to capsaicin, pH and also heat. For position N628, only the positively charged residues arginine and lysine were substitutions that resulted in temperature-specific phenotypes.

For the focused library, clones were selected as specific if 3 or 4 wells responded normally ($mean_{V1} - 2 \cdot \sigma_{V1} < response < mean_{V1} + 2 \cdot \sigma_{V1}$) to at least one, but hardly ($response < mean_{pcDNA} + 2 \cdot \sigma_{pcDNA}$) to another stimulus. Compared to the large-scale library the selection criteria were less strict, allowing the follow-up of relatively more clones. 19 clones were selected as hits, regrown and Maxi-prep DNA prepared. Full EC_{50} curves were measured for respective stimuli (n=3). 4 clones (N652Q/L/T and Y653T) were confirmed as hits and fully sequenced. Finally, we selected the three mutations N628K, N652T and Y653T with the strongest phenotypes for detailed analysis.

Detailed FLIPR temperature-activation curves were produced as described before30. Unnormalized fluorescence counts (F) were averaged and background (pcDNA) subtracted. Data points with a linear relationship in Log(F)-1/T plots were used to fit Boltzmann curves.

Molecular modeling

The rat TRPV1 homology model has been built from Kv1.2 (Protein Database accession number 2A79)31 as template as described before30.

Electrophysiology

HEK293 cells were co-transfected with EGFP and wild-type or mutant rTRPV1 constructs in wells of 24-well plates using Fugene 6.0 (Roche). Cells were reseeded on 12 mm round glass coverslips (Warner Instruments) one day after transfection. Recordings were

performed the following two days. Recording pipettes were pulled from micropipette glass (Sutter) and had 2–4 MΩ resistance. Whole-cell recordings were performed with pipette solution containing 150 mM NaCl, 3 mM $MgCl_2$, 5 mM EGTA, 10 mM HEPES; pH 7.2 and bath solution containing 150 mM NaCl, 6 mM CsCl, 1.5 mM $CaCl_2$, 1 mM $MgCl_2$, 10 mM glucose, and 10 mM Hepes; pH 7.4. Isolated cells were voltage-clamped in the whole-cell mode using an EPC9 (HEKA Instruments Inc) amplifier. Single-channel recordings were performed in the cell-attached configuration with a bath solution of 120 mM KCl, 5 mM Hepes, 1 mM $MgCl_2$ and 2 mM $CaCl_2$; pH 7.4 and a pipette solution containing 100 mM KCl, 10 mM Hepes, 1 mM $MgCl_2$ and 10 mM EGTA; pH 7.4. Voltage commands were made from the Pulse and PulseFit program, and the currents were filtered at 2.9 kHz and recorded at 5 kHz. Cells were continuously perfused with the bath solution through a Valve-Bank perfusion system (Automate Scientific). Temperature was controlled using a CL-100 temperature controller (Warner Instruments) and an SC-20 Solution In-Line Heater/Cooler (Harvard Apparatus) and measured with a thermistor placed in proximity to cell. All temperature-controlled experiments were performed within 1°C of the target temperature.

Whole-cell voltage-current experiments were only performed on patches with gigaseal resistances and voltage-steps were applied 3 (capsaicin) or 5 (temperature) times for each cell and condition. Plateau currents were calculated by averaging over the last 10 ms of each step. Current-voltage curves were leak-subtracted and normalized by the driving force to calculate conductance curves. The data were fitted in Igor Pro with a sigmoid curve to obtain the voltage values of half-maximal activation (V_{half}). V_{half} values of converging fits were subsequently averaged for each condition. Finally, averages and standard deviations from all cells were calculated. Current-rises and -decays upon voltage-steps at different temperatures were well-fit by single exponential curves that yielded time constants. Averages and standard deviations of time constants were calculated from multiple patches.

Current deflections from the baseline level were observed in TRPV1 or mutant transfected cells at high voltages or during application of capsaicin, but absent in pcDNA transfected cells in the presence of capsaicin or at high voltages. Single-channel recordings were analyzed with Igor Pro and QuB42-43. For determining single-channel amplitudes short sections of two distinct current amplitudes were selected, amplitude histograms calculated and fitted with two Gaussian curves. Single-channel amplitudes were calculated from the difference between the midpoints of the Gaussian fits and the standard deviation was taken from the broader of the two distributions (usually the open state). Current traces were idealized by using the half-amplitude method and closed- and open-time histograms calculated using the MIL algorithm of QuB and fitted with Igor Pro.

Supplementary Material

Refer to Web version on PubMed Central for supplementary material.

Acknowledgements

We thank Anthony Marelli and Tony Orth for preparing mini-prep DNA, Michael Caterina for providing ratTRPV1 plasmid DNA and Bertrand Coste for critical reading of the manuscript. This research was supported by NIH, Novartis Research Foundation, and a fellowship to J.G. from the American Heart Association.

References

1. Caterina MJ. Transient receptor potential ion channels as participants in thermosensation and thermoregulation. Am J Physiol Regul Integr Comp Physiol. 2007; 292:R64–76. [PubMed: 16973931]
2. Dhaka A, Viswanath V, Patapoutian A. Trp ion channels and temperature sensation. Annu Rev Neurosci. 2006; 29:135–161. [PubMed: 16776582]
3. Dhaka A, et al. TRPV1 is activated by both acidic and basic pH. J Neurosci. 2009; 29:153–158. [PubMed: 19129393]
4. Brauchi S, Orio P, Latorre R. Clues to understanding cold sensation: thermodynamics and electrophysiological analysis of the cold receptor TRPM8. Proceedings of the National Academy of Sciences of the United States of America. 2004; 101:15494–15499. [PubMed: 15492228]
5. Caterina MJ, et al. The capsaicin receptor: a heat-activated ion channel in the pain pathway. Nature. 1997; 389:816–824. [PubMed: 9349813]
6. Tominaga M, et al. The cloned capsaicin receptor integrates multiple pain-producing stimuli. Neuron. 1998; 21:531–543. [PubMed: 9768840]
7. Voets T, et al. The principle of temperature-dependent gating in cold- and heat-sensitive TRP channels. Nature. 2004; 430:748–754. [PubMed: 15306801]
8. Caterina MJ, et al. Impaired nociception and pain sensation in mice lacking the capsaicin receptor. Science (New York, N.Y. 2000; 288:306–313.
9. Davis JB, et al. Vanilloid receptor-1 is essential for inflammatory thermal hyperalgesia. Nature. 2000; 405:183–187. [PubMed: 10821274]
10. Guler AD, et al. Heat-evoked activation of the ion channel, TRPV4. J Neurosci. 2002; 22:6408–6414. [PubMed: 12151520]
11. McKemy DD, Neuhausser WM, Julius D. Identification of a cold receptor reveals a general role for TRP channels in thermosensation. Nature. 2002; 416:52–58. [PubMed: 11882888]
12. Peier AM, et al. A TRP channel that senses cold stimuli and menthol. Cell. 2002; 108:705–715. [PubMed: 11893340]
13. Peier AM, et al. A heat-sensitive TRP channel expressed in keratinocytes. Science (New York, N.Y. 2002; 296:2046–2049.
14. Smith GD, et al. TRPV3 is a temperature-sensitive vanilloid receptor-like protein. Nature. 2002; 418:186–190. [PubMed: 12077606]
15. Story GM, et al. ANKTM1, a TRP-like channel expressed in nociceptive neurons, is activated by cold temperatures. Cell. 2003; 112:819–829. [PubMed: 12654248]
16. Xu H, et al. TRPV3 is a calcium-permeable temperature-sensitive cation channel. Nature. 2002; 418:181–186. [PubMed: 12077604]
17. Talavera K, et al. Heat activation of TRPM5 underlies thermal sensitivity of sweet taste. Nature. 2005; 438:1022–1025. [PubMed: 16355226]
18. Togashi K, et al. TRPM2 activation by cyclic ADP-ribose at body temperature is involved in insulin secretion. The EMBO journal. 2006; 25:1804–1815. [PubMed: 16601673]
19. Gavva NR, et al. Molecular determinants of vanilloid sensitivity in TRPV1. The Journal of biological chemistry. 2004; 279:20283–20295. [PubMed: 14996838]
20. Jordt SE, Julius D. Molecular basis for species-specific sensitivity to “hot” chili peppers. Cell. 2002; 108:421–430. [PubMed: 11853675]
21. Jordt SE, Tominaga M, Julius D. Acid potentiation of the capsaicin receptor determined by a key extracellular site. Proceedings of the National Academy of Sciences of the United States of America. 2000; 97:8134–8139. [PubMed: 10859346]
22. Ryu S, Liu B, Yao J, Fu Q, Qin F. Uncoupling proton activation of vanilloid receptor TRPV1. J Neurosci. 2007; 27:12797–12807. [PubMed: 18032651]
23. Ahern GP, Brooks IM, Miyares RL, Wang XB. Extracellular cations sensitize and gate capsaicin receptor TRPV1 modulating pain signaling. J Neurosci. 2005; 25:5109–5116. [PubMed: 15917451]

24. Salazar H, et al. A single N-terminal cysteine in TRPV1 determines activation by pungent compounds from onion and garlic. Nature neuroscience. 2008; 11:255–261. [PubMed: 18297068]
25. Nilius B, et al. Gating of TRP channels: a voltage connection? The Journal of physiology. 2005; 567:35–44. [PubMed: 15878939]
26. Voets T, Owsianik G, Janssens A, Talavera K, Nilius B. TRPM8 voltage sensor mutants reveal a mechanism for integrating thermal and chemical stimuli. Nature chemical biology. 2007; 3:174–182. [PubMed: 17293875]
27. Latorre R, Brauchi S, Orta G, Zaelzer C, Vargas G. ThermoTRP channels as modular proteins with allosteric gating. Cell calcium. 2007; 42:427–438. [PubMed: 17499848]
28. Matta JA, Ahern GP. Voltage is a partial activator of thermo-sensitive TRP channels. The Journal of physiology. 2007
29. Brauchi S, Orta G, Salazar M, Rosenmann E, Latorre R. A hot-sensing cold receptor: C-terminal domain determines thermosensation in transient receptor potential channels. J Neurosci. 2006; 26:4835–4840. [PubMed: 16672657]
30. Grandl J, et al. Pore region of TRPV3 ion channel is specifically required for heat activation. Nature neuroscience. 2008; 11:1007–1013. [PubMed: 19160498]
31. Long SB, Campbell EB, Mackinnon R. Crystal structure of a mammalian voltage-dependent Shaker family K+ channel. Science (New York, N.Y. 2005; 309:897–903.
32. Liu B, Hui K, Qin F. Thermodynamics of heat activation of single capsaicin ion channels VR1. Biophysical journal. 2003; 85:2988–3006. [PubMed: 14581201]
33. Hille B. Ion Channels of Excittable Membranes. Ion Channels of Excittable Membranes. 2001
34. Premkumar LS, Agarwal S, Steffen D. Single-channel properties of native and cloned rat vanilloid receptors. The Journal of physiology. 2002; 545:107–117. [PubMed: 12433953]
35. Hui K, Liu B, Qin F. Capsaicin activation of the pain receptor, VR1: multiple open states from both partial and full binding. Biophysical journal. 2003; 84:2957–2968. [PubMed: 12719227]
36. Talavera K, Nilius B, Voets T. Neuronal TRP channels: thermometers, pathfinders and life-savers. Trends in neurosciences. 2008; 31:287–295. [PubMed: 18471901]
37. Kern D, Zuiderweg ER. The role of dynamics in allosteric regulation. Current opinion in structural biology. 2003; 13:748–757. [PubMed: 14675554]
38. Yang F, Cui Y, Wang K, Zheng J. Thermosensitive TRP channel pore turret is part of the temperature activation pathway. Proceedings of the National Academy of Sciences of the United States of America, PNAS. (in press).
39. Brauchi S, et al. Dissection of the components for PIP2 activation and thermosensation in TRP channels. Proceedings of the National Academy of Sciences of the United States of America. 2007; 104:10246–10251. [PubMed: 17548815]
40. Myers BR, Bohlen CJ, Julius D. A yeast genetic screen reveals a critical role for the pore helix domain in TRP channel gating. Neuron. 2008; 58:362–373. [PubMed: 18466747]
41. Bandell M, et al. High-throughput random mutagenesis screen reveals TRPM8 residues specifically required for activation by menthol. Nature neuroscience. 2006; 9:493–500. [PubMed: 16520735]
42. Qin F, Auerbach A, Sachs F. Estimating single-channel kinetic parameters from idealized patch-clamp data containing missed events. Biophysical journal. 1996; 70:264–280. [PubMed: 8770203]
43. Qin F, Auerbach A, Sachs F. Maximum likelihood estimation of aggregated Markov processes. Proceedings. 1997; 264:375–383.

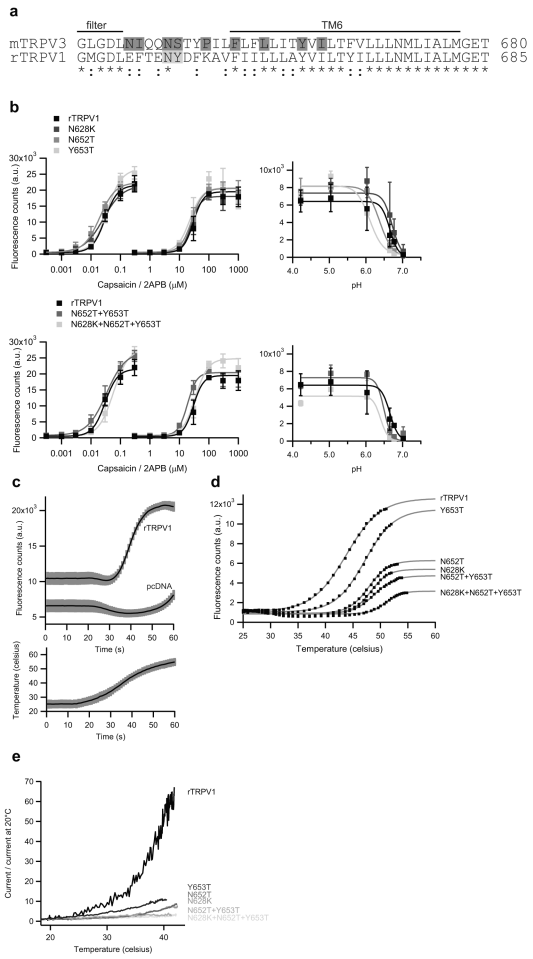

Fig. 1.

Chemical, acid and temperature responses of TRPV1 and point mutants.

a, Alignment of mouse TRPV3 and rat TRPV1 sequences. Predicted locations of selectivity-filter and TM6 are indicated with bars above the sequences. Residues found in TRPV3 to be specifically required for temperature-activation are highlighted in dark grey. Temperature-specific TRPV1 residues identified in the targeted screen are highlighted in light grey. Stars and colons indicate identical and homologous residues, respectively.

b, Average fluorescence counts from HEK293 cells expressing wild-type rTRPV1 and mutant channels in FLIPR fluo-3 assay in response to capsaicin, 2APB and acidic buffer. Values are averages of maximal responses (n=8 wells), error bars are s.d. c, An example of raw data of rTRPV1 and pcDNA transfected HEK293 cells in FLIPR temperature assay upon a heat stimulus (shown below). Solid lines are average values (n=28), gray bands indicate standard deviations. d, Background (pcDNA)-subtracted average fluorescence of wild-type and mutant transfected HEK293 cells loaded with fluo-3 in response to temperature stimulus as shown in c. Grey lines are Boltzmann fits to the data points (n=28). The temperature of half-maximal activation or efficacy-temperature (ET_{50}) is 43.8 ± 0.1°C (wild-type TRPV1), 48.3 ± 0.2°C (N628K), 47.9 ± 0.3°C (N652T), 47.2 ± 0.1°C (Y653T), 48.9 ± 0.3°C (N652T+Y653T), and 51.0 ± 0.3°C (N628K+N652T+Y653T). The maximum responses when normalized to wild-type TRPV1 (100 ± 21%) are 39 ± 11% (N628K), 47 ±

12% (N652T), 34 ± 9% (N652T+Y653T) and 20 ± 6% (N628K+N652T+Y653T). e, Whole-cell currents of cells transfected with wild-type TRPV1 or mutant receptors at +60 mV upon application of temperature-ramps.

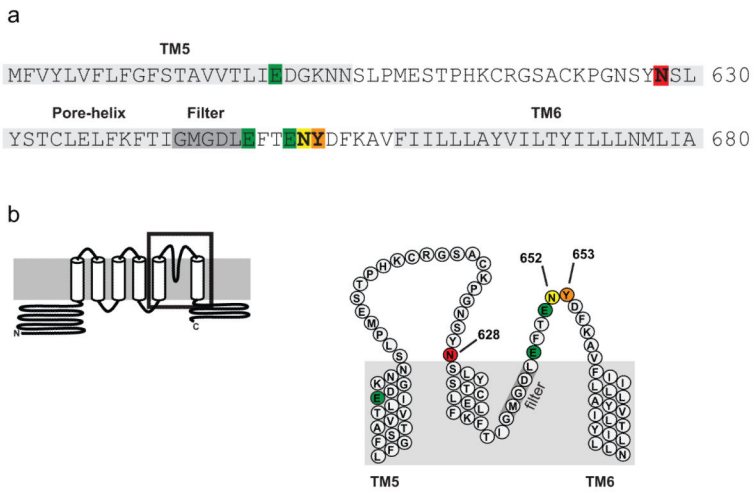

Fig. 2.

Location of point mutations.

a, Amino acid sequence of putative pore region of rTRPV1. Predicted locations of TM5 and TM6, the pore-helix and selectivity filter are highlighted in grey. Temperature-specific residues are highlighted red (N628), yellow (N653) and orange (Y653). Previously identified residues involved in acid-sensitivity are colored green. b, Schematic membrane topology of one subunit (left) and pore domain (right). Amino acids are colored as above.

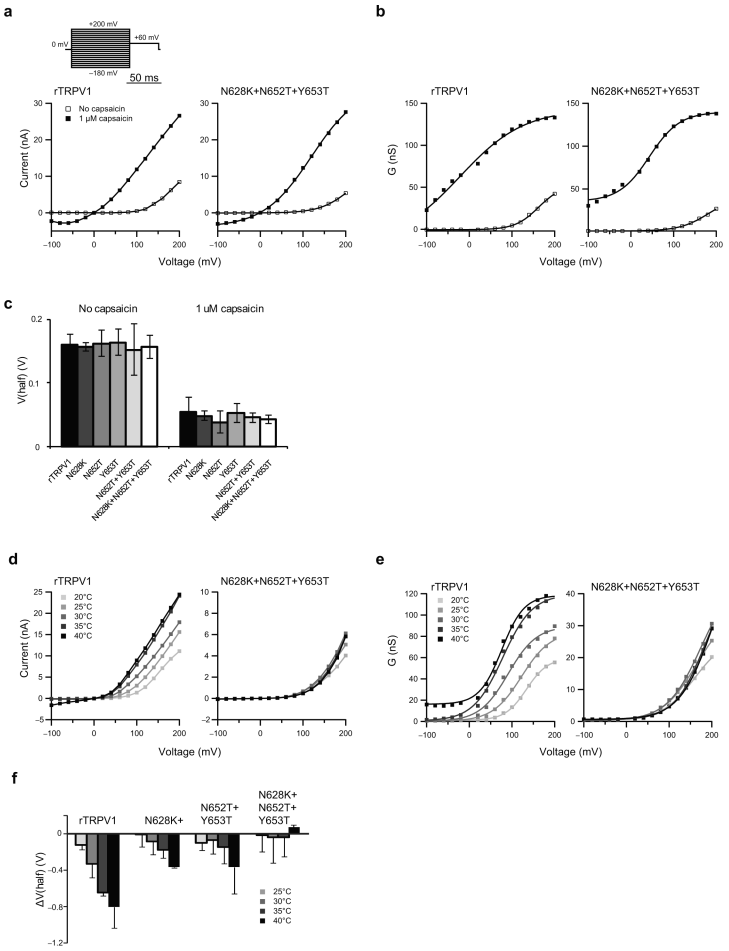

Fig. 3.

Voltage-activation of wild-typeTRPV1 and point mutants at different temperatures and during capsaicin-activation.

a, Voltage-step protocol applied to whole-cell patches of HEK293 cells transfected with rTRPV1 or triple-mutant (N628K+N652T+Y653T) cDNA in the absence or presence of 1 μM capsaicin at 20°C, pH 7.4 and typical examples of respective raw current-voltage (*I-V*) curves. b, Conductance-voltage (*G*-V) curves obtained from (*I-V*) curves shown in a. Lines are Boltzmann fits to the data. c, Averaged V_{half}-values of TRPV1 and point mutants in the absence of capsaicin (20°C, pH 7.4) and during application of 1 μM capsaicin; n=9 from 3 individual cells; errors are s.d.

d, Typical examples of raw current-voltage (*I-V*) curves obtained from voltage-step protocols applied to whole-cell patches of HEK293 cells transfected with rTRPV1 or triple-mutant (N628K+N652T+Y653T) cDNA at different temperatures. e, Conductance-voltage (*G*-V) curves obtained from (*I-V*) curves shown in d. Lines are Boltzmann fits to the data. f, Shifts in V_{half}-values evoked by different temperatures when compared to 20°C. n=15 from 3 individual cells; errors are s.d.

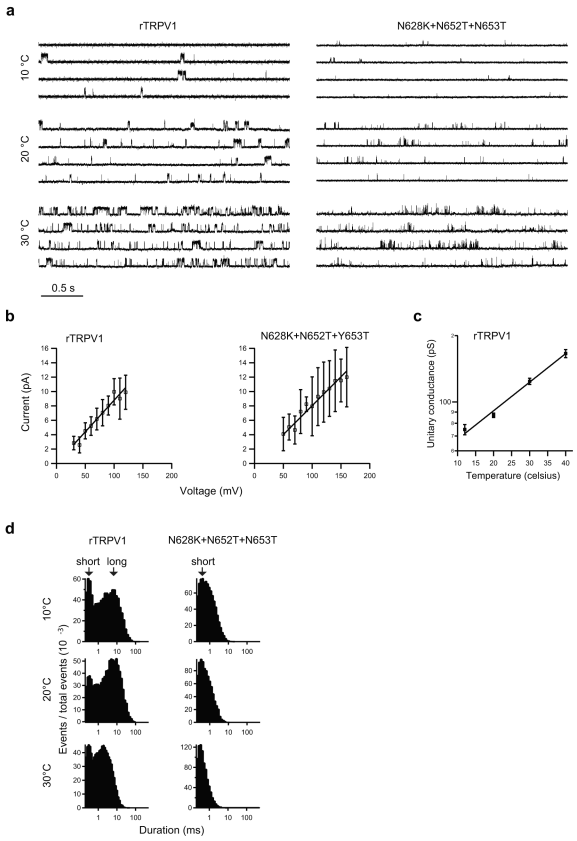

Fig. 4.

Single-channel currents of TRPV1 and triple mutant at different temperatures.

a, Examples of cell-attached current-recordings taken at +100 mV from cells transfected with rTRPV1 wild-type and the triple mutant (N628K+N652T+Y653T) at 10°C, 20°C an d 30°C. Upward deflections are channel openings; currents are filtered at 2.9 kHz. More example recordings are shown in Supplementary Fig. 4. b, Current-voltage relationship obtained from current-amplitude histograms of single-channel recordings at different voltages at 20°C. Error bars are s.d. from the broader peak of current-amplitude histograms. Lines are linear fits to the data. c, Unitary conductance of wild-type TRPV1 as a function of temperature. Average values are from current-amplitude histograms of single-channel recordings. Error bars are s.d. from the broader peak of current-amplitude histograms. The solid line is an exponential fit to the data. c, Open-time histograms of single-channel current traces at different temperatures. Each histogram is normalized to unity and represents 20.000–60.000 gating events. Arrows indicate the distinct short and long populations in wild-type TRPV1 and short population in the triple mutant (N628K+N652T+Y653T).

Table 1

Fit values from Hill-fits to capsaicin, 2APB and acid dose-responses.

	capsaicin		2APB		acid	
	EC_{50} (nM)	**Max. (a.u.)**	**EC_{50} (μM)**	**Max. (a.u.)**	**EC_{50}**	**Max. (a.u.)**
rTRPV1	30.1 ± 6.0	21541 ± 2120	29.8 ± 8.4	19503 ± 1220	6.7 ± 0.3	5532 ± 567
N628K	26.0 ± 6.0	21494 ± 1120	25.6 ± 6.6	18032 ± 1180	6.7 ± 0.1	7022 ± 651
N652T	19.8 ± 4.0	22403 ± 1370	26.2 ± 7.0	20534 ± 1590	6.5 ± 0.7	6549 ± 800
Y653T	35.5 ± 6.6	26671 ± 2080	22.6 ± 4.8	20379 ± 1690	6.2 ± 0.3	7308 ± 605
N652T+Y653T	33.2 ± 11.0	26866 ± 2500	18.8 ± 3.0	20407 ± 878	6.6 ± 1.9	6438 ± 584
N628K+N652T+Y653T	44.8 ± 12.0	24434 ± 1830	34.9 ± 7.2	24758 ± 1660	6.5 ± 0.1	4705 ± 365

EC_{50}-values and maximal responses from fits of the Hill-equation to the data shown in Fig. 1b. Errors are standard deviations of the fit values.